



Kinetics and Thermodynamic Study of Acid Red 73 Dye Removal on HCl- Water Hyacinth Stems Biomass



Hassan Ahmed EL-Adawy^{1,2}

¹Chemistry Department, Faculty of Science, AL-Azhar Univeristy, Cairo, 11884, (EGYPT)

²Chemistry Department, Faculty of Science, AL-Baha University, EL-Mukhwa, 1988, (KSA).

DYE containing waste water can cause serious water pollution problems by hindering light penetration and photo synthesis and toxicity from heavy metals associated with dyes. The ability of HCl-water hyacinth stems (HCl-WHS) biomass powder to adsorb acid red 73 (AR73) dye, from aqueous solutions has been investigated through batch experiments. The dye removal was found to be dependent on adsorbent dosage, initial dye concentration, mixing speed, contact time and adsorbent particle size. All batch experiments were carried out at constant pH and temperature of 3.0 and 289K respectively. Pseudo-first-order and pseudo-second-order models have been used to represent the process kinetics and obtain the main kinetic parameters. The results show that the pseudo-first order model is the one that best describes the biosorption of the AR73. The experimental isotherm was analyzed using the Langmuir and Freundlich equations. The maximum adsorption capacity was found 50 mg AR73 per g HCl-WHS powder. The thermodynamic study indicated that the adsorption of AR73 onto HCl-WHS surface was favorable, spontaneous and endothermic.

Keywords: Water hyacinth stems, Kinetics, Adsorption, Acid red 73 (AR73), Isotherms.

Introduction

Dyes are important water pollutants which are generally present in the effluents of the textile, leather, food processing, dyeing, cosmetics, paper, and dye manufacturing industries. They are synthetic aromatic compounds which are embodied with various functional groups [1]. The discharge of toxic effluents from various industries adversely affects water resources, soil fertility, aquatic organisms and ecosystem totality. Appearance of colour in effluents is one of the major problems encountered in the textile industry. The textile waste water is rated as the most polluting among all in the industrial sectors [2,3]. The textile industry consumes large amounts of water and produces large volumes of wastewater through various steps in dyeing and finishing processes. The textile waste water

is a complex and variable mixture of pollutants like organic, inorganic, elemental and polymeric materials [4]. The textile wastewater containing azo-dyes are some of the most disobedient classes of organic compounds to treat, due to their azo groups usually attached to radicals, of which at least one is an aromatic group [5, 6]. It is well known that some azo-dyes and their degradation products are highly carcinogenic. Colored waste waters in the ecosystem are a source of aesthetic pollution, of eutrophication, and of perturbations in aquatic life [7]. Due to low biodegradation of dyes, convectional biological treatment process is not very effective in treating dye wastes. The usual treatment processes like physical and chemical methods like adsorption, flocculation, coagulation, radiation, etc [8]. Among all the methods, adsorption is one of the most effective method of dyes removing from waste effluents

*Corresponding author e-mail: hassan_el.adawi@yahoo.com

Tel:+966565933731; ORCID: 0000-0002-5480-5002

Received 22/3/2019; Accepted 1/10/2019

DOI :10.21608/ejchem.2019.11026.1707

©2020 National Information and Documentation Center (NIDOC)

[9, 10]. Granular or powdered activated carbon is the most widely used adsorbent because it has an excellent adsorption capacity for organic compounds, but its use may be restricted due to its high cost [11]. This has led many searchers to search for another sources to prepare activated carbons or cheaper substitutes such as fly ash, silica gel, wool wastes, blast furnace slag, and clay materials.

In Egypt, *Eichhornia crassipes* (E.C.) (Water hyacinth), can be found in great water areas in the ponds and lakes. Due to its vigorous growth rate, can effect water flow, prevent sunlight from reaching aquatic plants, forbid the water of oxygen, leading to killing fish and also acts as a main habitat for mosquitoes. Its massive biomass production rate, its high possibility to pollution, and its heavy metal absorption capacities, [12,13] qualify it for use in wastewater treatment. The ability of water hyacinth (*Eichhornia crassipes*) to remove heavy metals in solution is well documented [14]. Considering the uses and applications of the water hyacinth in various above mentioned concepts, its major role in textile effluent treatment is recently undergoing higher attention to find an alternative for the currently available textile effluent treatment techniques. Thus, the present review deals with the adsorption capacity of the HCl-water hyacinth stems for the treatment of textile waste water in textile industrial effluents.

Materials and Methods

Preparation of the HCl-WHS

Water hyacinth was collected from the Manzala Lake, Dakahlia governorate of Egypt. The spongy stems of collected Water hyacinth were separated from roots and leaves and washed thoroughly with tap water several times to remove earthy matter and finally cut to small pieces. The sliced material was dried in sunlight for 7 days and subsequently at 70°C for 2 h in oven. The dried material was milled into a powder using domestic mixer and was allowed to pass through a 10 to 80 mesh opening size sieves. The sieved powder was treated with 1% HCl for 24 h. After that, the samples were filtered and rinsed well with distilled water. The treated material was dried again at 70°C for 2 h, packed in plastic bags, and stored for use.

Preparation of Adsorbate Solution

AR73 (molecular weight: 656.5 g/mol, λ_{\max} : 545 nm, CI 27290, chemical formula $C_{22}H_{14}N_4$

$Na_2O_7S_2$) was obtained from Merck and used without purifications, their chemical structure is illustrated in Fig.1. A calculated amount of the dye (500 mg/L) was dissolved separately in 1.0 L of distilled water to prepare stock solution. For batch study, an aqueous solution of this dye was prepared from stock solution in distilled water. NaOH and HCl solutions were used to adjust pH.

Effect of Contact Time and Initial Dye Concentration

The effect of contact time of adsorbent (HCl-WHS) was studied at 5, 15, and 25 mg/L initial concentration of dye solution. A constant mass 0.06 g of adsorbent was mixed with a 20 mL dye solution at 3.0 pH. The mixture of each batch was constantly agitated as a function of time at speed of 800 rpm and controlled temperature 298K. At various time intervals (15, 30, 45, 60, 75, and 90 minutes), samples were taken and filtered to remove the adsorbent, then the dye concentrations were measured by UV-Vis Spectrophotometer.

Effect of pH

The solution pH was adjusted between 3.0 and 12 by the addition of 1% HCl or 1% NaOH. In this study, 20 ml of 25 mg/L dye solution was agitated with 0.06 g of HCl- WHS at 298 K and at a constant speed of 800 rpm. Samples were then analyzed using UV-Vis Spectrophotometer.

Effect of Adsorbent Dosage

Initial dye concentration of 25 mg/L were used in conjunction with adsorbent dose of 1.0 to 5.0 g/L. Contact time, pH, agitation speed, temperature and particle size of 90 minutes, 3.0, 800 rpm, 298 K and 420-595 μm respectively were kept constant.

Effect of Agitation Speed

The effect of agitation speeds is carried out at 200, 400, 600, 800 and 1000 rpm in conjunction with initial dye concentration of 25 mg/L. Adsorbent dose, pH, temperature, contact time and particle size of 3.0 g/L, 3.0, 298 K, 90 minutes and 595-841 μm respectively were kept constant.

Effect of Particle Size

The effect of particle size is conducted at four sizes of 297- 420, 420-595, 595-841 and 841-2000 μm in conjunction with 25 mg/L of AR73 concentration. Contact time = 90 minutes, adsorbent dose = 3.0 g/L, agitation speed = 800 rpm, temperature = 298 K and pH = 3.0 were kept constant.

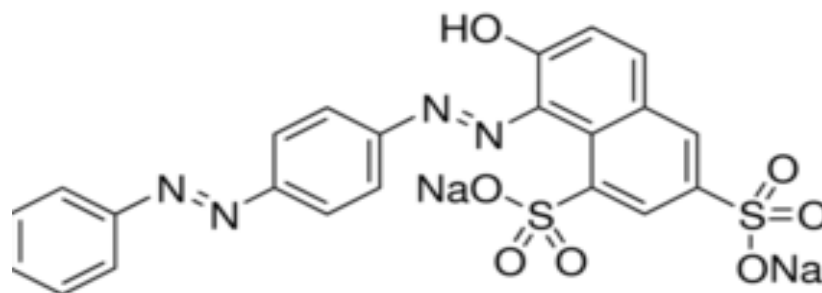


Fig. 1. Chemical structure of acid red 73 (AR73).

Effect of Temperature

288, 303, 313 and 323K temperatures were used in conjunction with 25 mg/L of AR73 concentration. Contact time=90 minutes, adsorbent dose 3.0 g/L, pH =3, agitation speed= 800 rpm and particle size 595-841 μ m were kept constant.

Adsorption Models

The adsorption isotherms show how the molecules of adsorbate distribute between the solid and liquid phase when the adsorption process reaches an equilibrium state. The Langmuir and Freundlich isotherm equations are usually employed for the solid-liquid systems. The Langmuir theory assumes that, adsorption include the attachment of only one molecular monolayer on adsorbent surface and the ions are adsorbed on a fixed number of well-defined sites, each site can hold one ion, all sites are energetically equivalent and there is no interaction between the ions [15, 16]. The analysis of the isotherm data is important to determine the adsorption capacity of the adsorbent [17].

The form of Langmuir isotherm [18] can be given by the following equation (1):

$$\frac{C_e}{q_e} = \frac{1}{q_m b} + \frac{C_e}{q_m} \quad (1)$$

Where q_e is the amount of dye adsorbed on the adsorbent at equilibrium (mg/g); C_e is the concentration of dye at equilibrium (mg/L); q_m is the maximal amount of dye adsorbed onto the adsorbents (mg/g); and K_L is the Langmuir constant of adsorption (L/mg). The essential characteristic of the Langmuir isotherm can be evidenced by the dimensionless constant called equilibrium parameter, R_L (2).

$$R_L = \frac{1}{1 + K_L C_0} \quad (2)$$

Where K_L is the Langmuir constant and C_0 is the initial AR73 concentration. R_L values indicate the type of isotherm to be irreversible ($R_L = 0$), favorable ($0 < R_L < 1$), linear ($R_L = 1$) or unfavorable ($R_L > 1$) [19].

The Freundlich model assumes that the sorption take place on heterogeneous surfaces and adsorption capacity depends on the concentration of molecules at equilibrium. The Freundlich model equation is conveniently used in the linear form as:

$$q_e = k_f C_e^{1/n} \quad (3)$$

A linear form of this expression is:

$$\ln q_e = \ln k_f + 1/n \ln C_e \quad (4)$$

$1/n$ and k_f (mg g^{-1}) are empirical Freundlich constants and indicate adsorption capacity and intensity, respectively. Their values were obtained from the intercepts ($\ln k_f$) and slopes ($1/n$) of linear plots of $\ln q_e$ versus $\ln C_e$.

Thermodynamic Parameters

Thermodynamic parameters are important in the design of adsorption process. The thermodynamic parameters were determined by using following equations:

$$\Delta G^\circ = -RT \ln K_d \quad (5)$$

$$K_d = \frac{C_a}{C_e} \quad (6)$$

$$\ln K_d = \frac{\Delta G^\circ}{R} + \frac{\Delta H^\circ}{RT} \quad (7)$$

Where K_d is the distribution constant, C_a is the amount of dye adsorbed on the adsorbent

of the solution at equilibrium (mol/L), C_e is the equilibrium concentration, R is the gas constant ($\text{J}\cdot\text{mol}^{-1}\cdot\text{K}^{-1}$), T is absolute temperature (K), ΔH° is the standard enthalpy, ΔS° is the standard entropy and ΔG° is the free energy.

Adsorption Kinetics

To investigate the kinetics of biosorption of AR73 onto HCl-WHS surface, two of the main models proposed in the literature have been selected to calculate the kinetic parameters. The pseudo-first order equation [20] (Lagergren, 1898), is generally expressed as follows:

$$\log(q_e - q_t) = \log q_e - \frac{k_1}{2.303} t \quad (8)$$

Where q_t and q_e are the amount adsorbed (mg/g) at time, t , and at equilibrium respectively and k_1 is the rate constant of the pseudo-first-order adsorption process (min^{-1}). k_1 and q_e values were determined from the slope and intercept of the plots of $\ln(q_e - q_t)$ versus t .

The linear form of pseudo second-order model is expressed as follows [21]:

$$\frac{t}{q_t} = \frac{1}{k_2 q_e^2} + \frac{t}{q_e} \quad (9)$$

Where k_2 is the pseudo second-order rate constant ($\text{g mg}^{-1} \text{min}^{-1}$). The values of q_e and k_2 were determined from the slope and intercept of the plot of t/q_t versus t .

Characterization

The surface morphology of HCl-WHS was examined by scanning electron microscopy, SEM Model Quanta 250 FEG (Field Emission Gun) attached with EDX Unit (Energy Dispersive X-ray Analyses), with accelerating voltage 30 K.V., magnification 14x up to 1000000 and resolution for Gun. 1nm).

Calculations

The amount of dye adsorbed at equilibrium q_e (mg/g) was calculated using the following equation:

$$q_e = \frac{(C_o - C_e)V}{W} \quad (10)$$

where C_o and C_e (mg/L) are concentrations of dye solution at initial and equilibrium respectively, V (L) the volume of the solution, and W (g) is the mass of the adsorbent used.

The amount of dye adsorbed at time t , q_t (mg/g), was calculated using:

$$q_t = \frac{(C_o - C_t)V}{W} \quad (11)$$

The extent of adsorption is expressed in percentage as removal efficiency (%R) and is calculated using:

$$\%R = \frac{(C_o - C_t)}{C_o} \times 100 \quad (12)$$

Result and Discussions

SEM Analysis

The surface morphology of HCl-WHS before and after adsorption of acid red 73 was shown in Fig. 2 (a & b). In the SEM micrograph 2 (a), shows the rough and porous surface of the adsorbent, which is one of the factors increasing adsorption capacity. The loaded SEM images, 2 (b), shows the adsorption of acid red 73 on the HCl-WHS. It is clearly seen that the caves, pores and surfaces of adsorbent were covered by the dye molecules. It is clear that upon adsorbing the acid red 73 dye molecules, the adsorbent structure has changed.

Effect of pH

It is evident from Fig. 3. that the process of adsorption of AR73 on HCl-WHS surface is highly dependent on the pH of the solution. The interaction between adsorbent and dye molecules is a combined result of charges on dye molecules and the adsorbent surface [22]. The removal capacity of acid red 73 decrease, with pH increasing. The maximum dye uptake has been observed at pH 3.0 (82.0 %) and thereafter the removal decreases. As at low pH, surface of HCl-WHS acquire positive charge and the presence of SO_3 groups in dye molecules is responsible for electrostatic attraction between positive charge surface and dye [23].

Effect of Adsorbent Dosage on Dye Uptake

Adsorbent dose is representing an important parameter that affecting on the adsorbent capacity at given initial concentration of adsorbate. It was observed from Fig. 4. That, the adsorption capacity of AR73 dye increased rapidly in the first stage with the increase in the adsorbent dose then increased slowly with the further increase in the adsorbent dose. The percent of dye uptake was noticed is 70.3% at adsorbent dose of 1.0 g/L and increase to 87.39 % with increase of adsorbent dose to 3.0 g/L. finally the dye percent removal

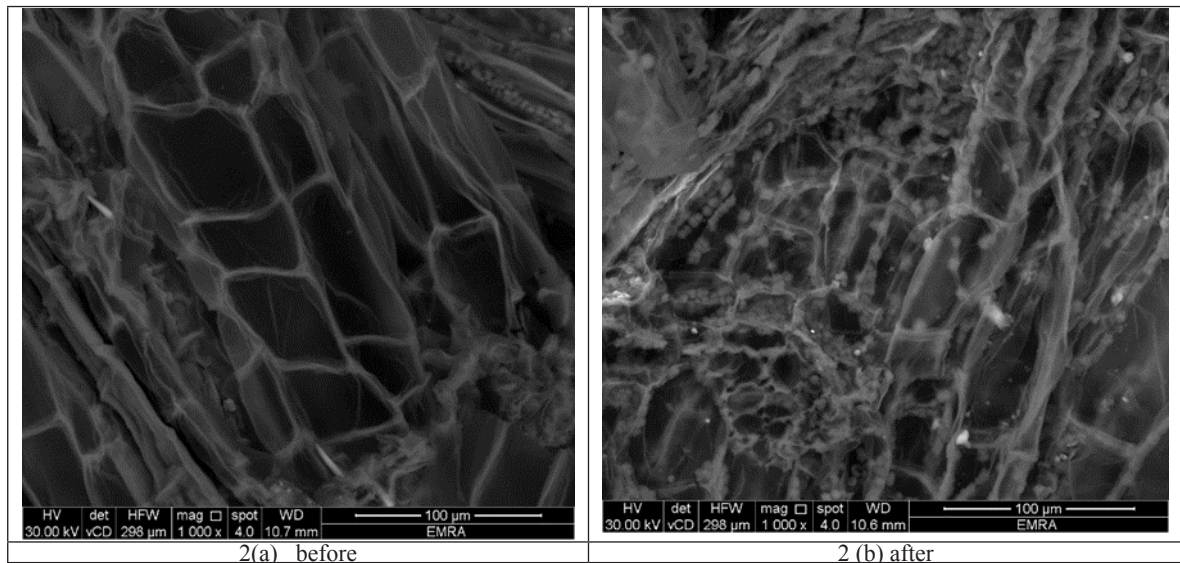


Fig. 2. SEM Micrograph of HCl-WHS before and after adsorption.

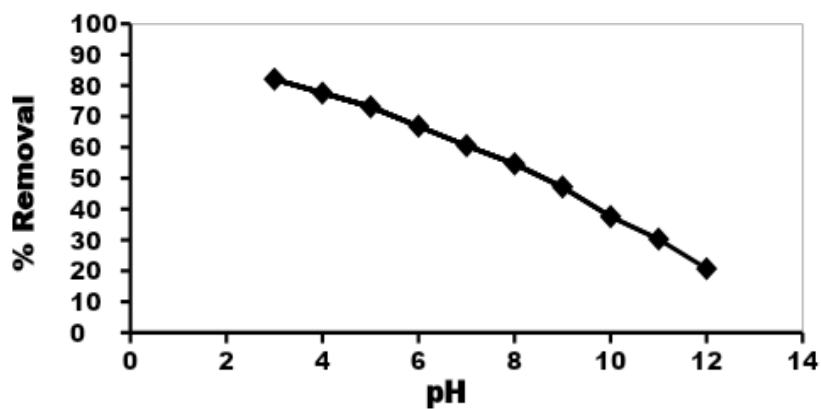


Fig. 3. Effect of pH on the adsorption of AR73 onto HCl-WHS surface ($C_i = 25$ mg/L, $T = 298$ K, dosage = 3.0 g/L)

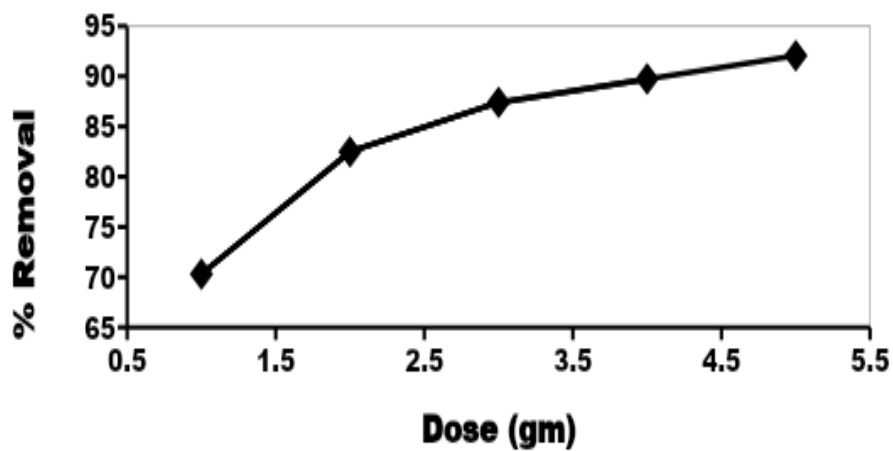


Fig. 4. Effect of adsorbent dose on the adsorption of AR73 onto HCl-WHS surface ($C_i = 25$ mg/L, $T = 298$ K, pH = 3.0).

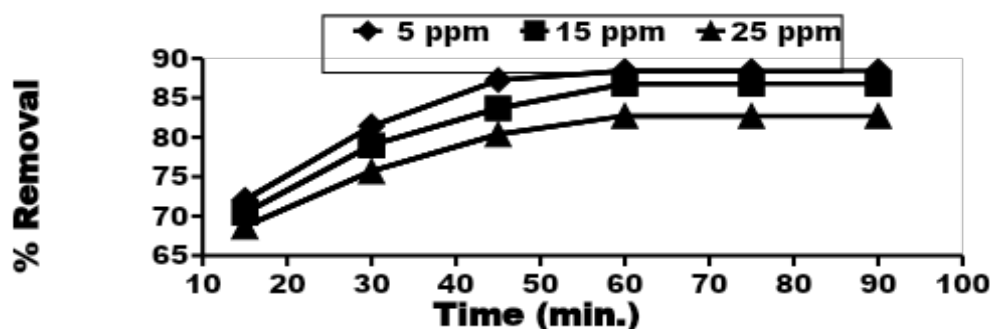


Fig. 5. Effect of contact time and initial dye concentration on the adsorption of AR73 onto HCl-WHS surface (Dosage = 3.0 gm/L, T = 298K, pH = 3.0)

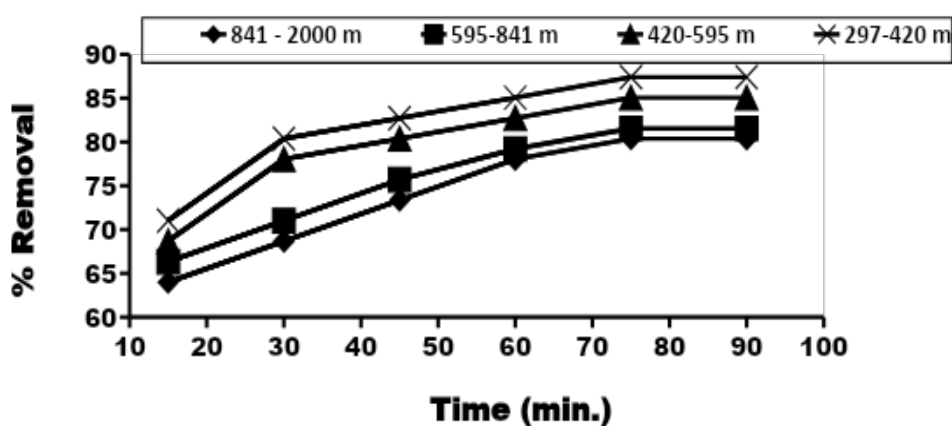


Fig. 6. Effect of adsorbent particle size on the adsorption of AR73 onto HCl-WHS surface ($C_i = 25$ mg/L, dosage = 3.0 gm/L, T = 298 K, pH = 3.0)

reaches only 89.7 % at 4.0 g/L of adsorbent, and therefore 3.0 g/L of adsorbent was chosen as the optimum dose and used in the further experiments. The increase in % removal of AR73 dye with the increase in the amount of HCl-WHS up to 4.0 g can be assigned to increase in both the surface area and the adsorption sites to AR73 dye molecules [24, 25].

Effect of Contact Time and Initial Dye Concentration

Fig. (5) Shows the effect of initial AR73 dye concentration on percent removal efficiency. It can be seen that the percentage removal decreased with increase in initial dye concentration from 5 to 25 ppm. This may be attributed to an increase in the driving force of the concentration gradient with the increase in the initial dye concentration [26]. The uptake of AR73 onto HCl-WHS was increased with the increase in contact time and the adsorption equilibrium was achieved at 90 min for AR73. The initial biosorption was rapid due to the adsorption of dye molecules onto exterior surface, after that dye molecules enter into inner pores a

relatively slow process [27].

Effect of Adsorbent Particle Size

The effect of particle size on the adsorption of AR73 onto HCl-WHS is shown in Fig. 6. Four particle size ranges were selected based on the sieve analysis, namely 297–420 μm , 420–595 μm , 595–841 μm and 841–2000 μm . From the Fig. 6 it is possible to conclude that as the particle size decrease, the percent of dye removal increase up to optimal point. This can probably be attributed to the presence of large number of smaller particles which provide a larger external surface area for dye adsorption at the initial stage [28]. On the other hand, at later stages of the experiment, the effect of particle size on dye removal was not prominent.

Effect of Temperature

The effect of temperature on adsorption of AR73 onto HCl-WHS was carried out at various temperatures including 288, 303, 318, and 333 k. The results of this effect are given in Fig. 7, and shows the adsorption of dye tended to increase

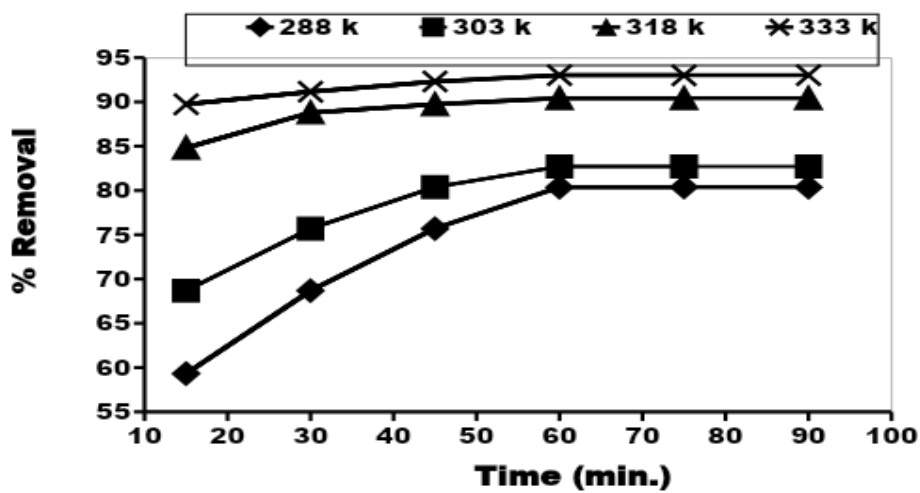


Fig. 7. Effect of temperature on the adsorption of AR73 onto HCl-WHS surface ($C_i = 25$ mg/L, dosage = 3.0 gm/L, pH = 3.0)

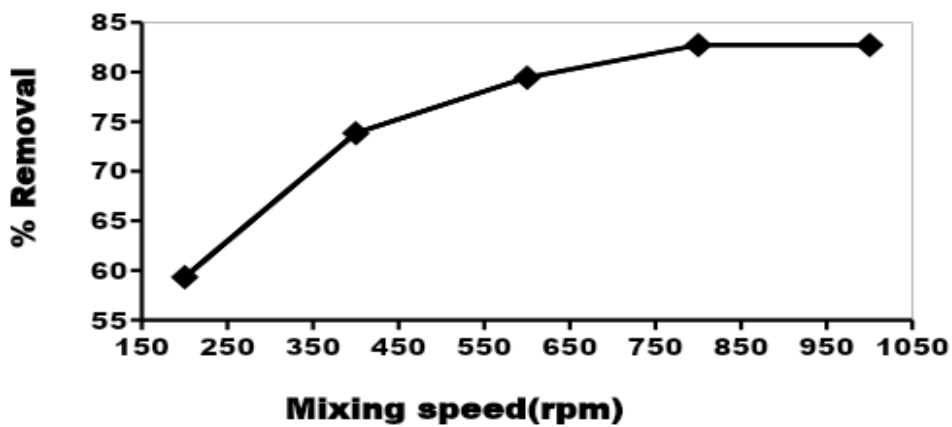


Fig. 8. Effect of mixing speed on the adsorption of AR73 onto HCl-WHS surface ($C_i = 25$ mg/L, dosage = 3.0 gm/L, T = 298 K, pH = 3.0).

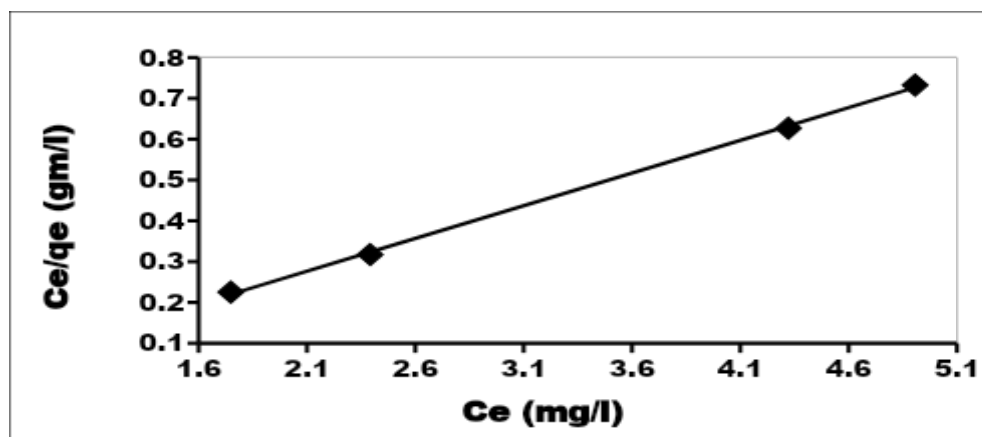


Fig. 9. Langmuir isotherm (T = 298 K, dosage = 3.0 g/L, $C_i = 25$ mg/L, pH = 3.0,).

TABLE 1. Isotherm parameters for adsorption of acid red 73 onto HCl-water hyacinth stems

q_m (mg/g)	K_L (L/ mg)	Langmuir		Freundlich		
		R^2	R_L	K_F (mg/g)	1/n	R^2
50	4.1	0.999	0.24	10.8	0.14	0.986

as increasing temperature. When the temperature increased gradually 288, 303, 318, and 333 k, the maximum adsorption capacities of AR73 removed by HCl-WHS is found to be increased as 80.3, 82.7, 90.4, and 93 % respectively. This is attributed to the increase in the rate of intra-particle diffusion of dye molecules into the porous structure of adsorbent as increase of temperature, as well as diffusion is an endothermic process so the adsorption increases with temperature. Besides, increasing temperature might also produce a swelling effect within the internal structure of adsorbent enabling more dye molecules diffuse into HCl-WHS.

Effect of Mixing Speed

The adsorption process is influenced by mass transfer parameters. The adsorption of AR73 by HCl-WHS at different mixing speeds ranging from 200 to 1000 rpm was studied. As shown in Fig. 8, the percentage of dye removed at was found to increase from 59.3, 79.4 and 82.7 % with increased in mixing speed from 100, 600 and 800 rpm. This is attributed to with low mixing speed the greater contact time is required to achieve the equilibrium, while with increasing the mixing speed, the rate of diffusion of adsorbate molecules from bulk liquid to the liquid boundary layer surrounding the particles become higher due to an enhancement of turbulence and a decrease of thickness of the liquid

boundary layer.

Adsorption Isotherm

As shown in Figs. 9 & 10, the models of Langmuir and Freundlich were employed to study the adsorption isotherms of AR73 dye. The maximum adsorption capacity (q_m) and Langmuir constant (K_L) were calculated from the plot between C_e and C_e/q_e , the results were summarized in Table 1.

The results show that the correlation value of R^2 obtained from Langmuir isotherm equation (0.999) was higher than from Freundlich (0.986) indicates that the adsorption AR73 by HCl-WHS can be adequately modeled by the Langmuir and which indicate that adsorption of AR73 was made up homogenous surface and monolayer adsorption. The maximum capacity of uptake for AR73 removal by HCl-WHS was higher with 50.0 mg/g. The separation factor R_L is 0.24, showing that the adsorption of AR73 on HCl-WHS surface is favorable.

Thermodynamics

The thermodynamic parameters (ΔG° , ΔH° and ΔS°) are reported in Table 2, the negative values of ΔG° indicated that the biosorption process was favorable and spontaneous in nature for AR73 dye. It may be noted that with the increase of temperature from 288 K to 333 K, the value of

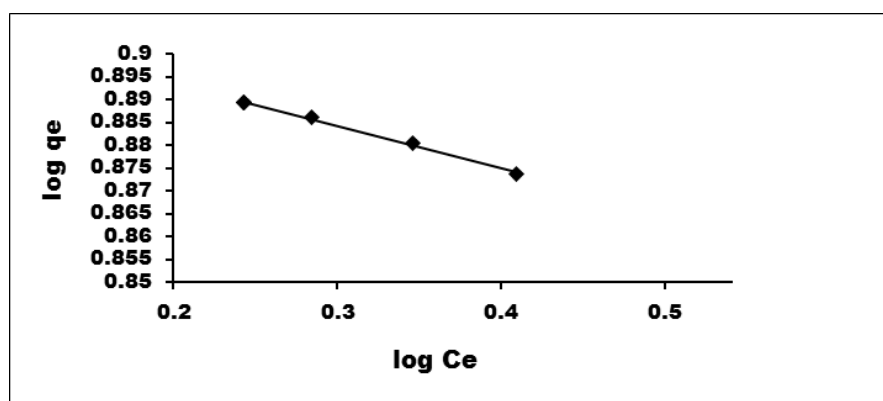


Fig. 10. Freundlich isotherm (T = 298 K, Dosage = 3.0 g/L, C_i = 25 mg/L, pH =3.0,).

TABLE 2. Thermodynamic parameter for adsorption of acid red 73 onto HCl-water hyacinth stems surface

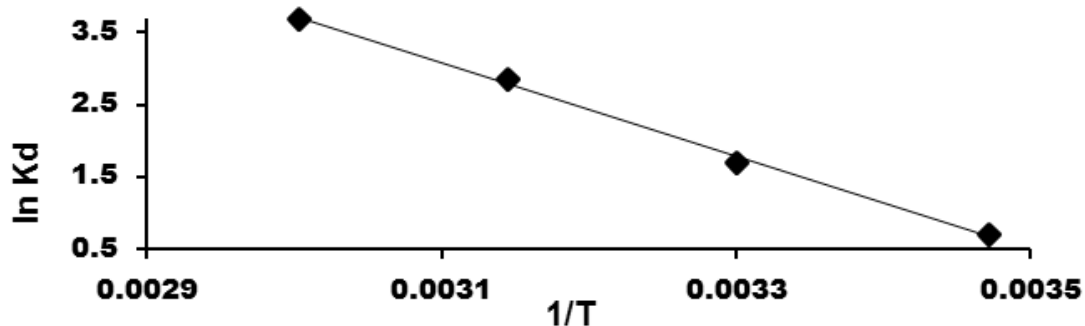
Adsorbent	Adsorbate	ΔH° (KJ.mol ⁻¹)	ΔS° (KJ.mol ⁻¹)	ΔG° (KJ.mol ⁻¹)			
				288 K	303K	318 K	333K
HCl-WHS	AR73	53.60	0.19	- 1.65	- 3.15	- 7.45	-10.15

TABLE 3. The pseudofirst-order and pseudosecond-order kinetic parameters for the adsorption of acid red 73 onto HCl-water hyacinth stems

C_0 (mgL ⁻¹)	q_e (exp.) (mg g ⁻¹)	Pseudo-first-order model			Pseudo-second-order model		
		k_1 (min ⁻¹)	q_e (cal.) (mg g ⁻¹)	R^2	K_2 (g mg ⁻¹ min ⁻¹)	q_e (cal.) (mg g ⁻¹)	R^2
5	1.47	0.038	1.5	0.9994	9.45	0.40	0.9591
15	4.33	0.024	4.55	0.9963	4.2	1.04	0.9996
25	13.1	0.025	13.8	0.9832	2.07	1.8	0.9996

TABLE 4. Comparison of the maximum adsorption capacity of AR73 on various adsorbents based on Langmuir model

Adsorbent	Adsorption capacity (mg/g)	References
Parthenium hysterophorus L	2.86	[30]
Magnetic nanoparticles Fe ₃ O ₄	40.1	[31]
copper diethyldithiocarbamate (Cu(DDTC) ₂)	42.9	[32]
chitosan	728.2	[33]
chitosan nano particles	1.25	[34]
HCl-water hyacinth stems (HCl-WHS)	50	This study

**Fig. 11. Von't Hoff plot for effect of temperature on adsorption of AR73 onto HCl-WHS**

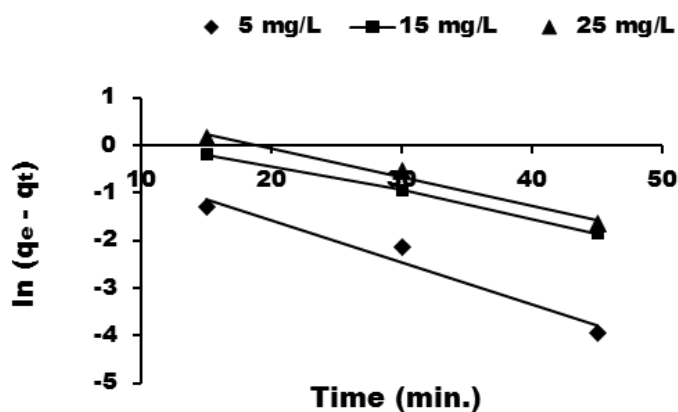


Fig. 12. Pseudo-first-order kinetics for AR73 adsorbed onto HCl-WHS at different concentrations.

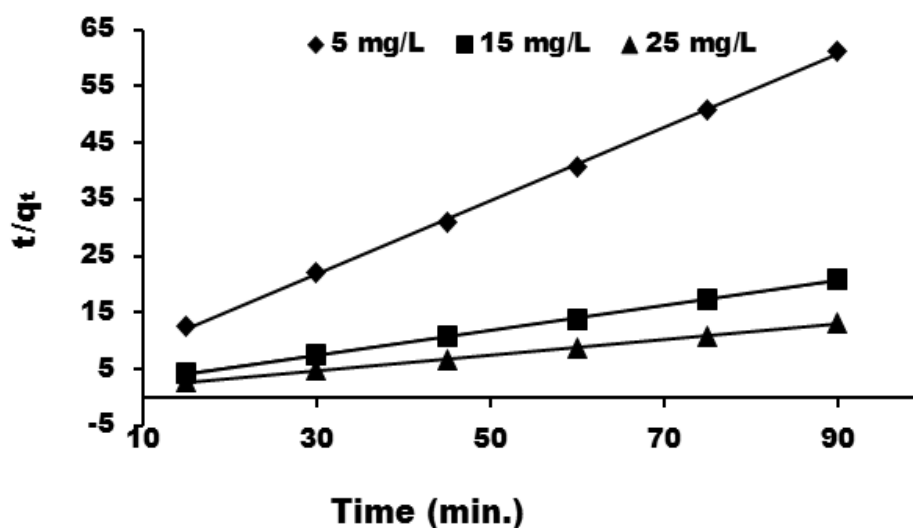


Fig. 13. Pseudo-second-order kinetics for AR73 adsorbed onto HCl-WHS at different concentrations.

ΔG° decreased from $-1.65 \text{ kJ mol}^{-1}$ to $-10.15 \text{ kJ mol}^{-1}$ for AR73 dye. Thus adsorption of AR73 dye onto HCl-WHS biomass was enhanced at higher temperature. Fig. 11 illustrates Von't Hoff plot of effect of temperature on adsorption of AR73 on HCl-WHS. The positive value of the enthalpy change (ΔH°) indicates that the adsorption process is endothermic and can be accepted to be a chemical in nature and involve strong forces of attraction because its value is more than 40 KJ/mol [29]. The positive value of ΔS° shows the increasing randomness at the solid/solution interface during adsorption of AR73 on the HCl-WHS surface and therefore a good affinity of the dye molecules towards the adsorbent.

Adsorption Kinetics

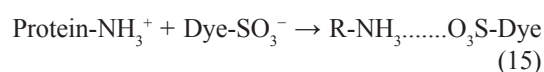
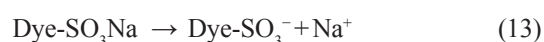
Egypt. J. Chem. Vol. 63, No. 4 (2020)

The capability of pseudo-first and second order kinetic models were examined in this study at three different initial concentration of AR73 dye (5, 15, and 25 mg/L) and at constant temperature of 298K was shown in Figs. (12, 13) and the data are listed in table 3. From the data in Table 3, it can be seen that, at all studied concentrations, the correlation coefficients R^2 of second order models are small in compare with that of first order model. Also, the experimental q_e values do not agree with the calculated ones, suggesting the non-applicability of the pseudo-second-order model to the adsorption processes of AR73 onto HCl-WHS. In this case, the fitting of the experimental data in the pseudo-first-order equation showed excellent linearity with high correlation coefficient ($R^2 >$

0.999). On the other hand, the calculated results of q_e by means of the pseudo first order model agreed perfectly with the experimental values at three initial concentrations, respectively. Therefore the kinetics of adsorption of AR73 onto HCl-WHS can be explained accurately by the pseudo-first-order kinetic model.

Suggested Mechanism

The possible mechanisms of the adsorption process of AR73 onto HCl-WHS in aqueous solution are likely to be ionic interactions of the dye ions with the amino groups of the protein present in the water hyacinth stems as the following steps:



First, the sulfonate groups of Acid Red 73 ionized in aqueous solution to anionic ions (Dye-SO_3^-) (13). In the presence of H^+ , the amino groups of water hyacinth proteins became protonated (protein-NH_3^+) (14). Then the adsorption proceeds according to the electrostatic attraction between these two counterions (15).

Comparison Study of AR73 Removal on Different Adsorbent Surfaces

Comparison of maximum monolayer adsorption capacities (based on the Langmuir adsorption isotherm model) of AR73 using various adsorbents were reported in Table 4. The results obtained experimentally in this work are higher than the results obtained by other studies. This clearly indicates that the HCl-WHS can be used as good adsorbent for acidic dye removal.

Conclusion

Adsorption method, using natural and agricultural waste materials to remove dyes from their aqueous solution shows an efficient and cost effective alternative compared to traditional chemical and physical techniques. This study investigated the adsorption of an acidic dye, acid red 73, onto HCl activated water hyacinth stems as a function of initial dye concentration, adsorbent dose, pH, mixing speed, particle size, and temperature. We found that (1) the adsorption equilibrium correlated fitted well with the Langmuir isotherm model, (2) the adsorption kinetics agree with first order model,

(3) thermodynamic results which indicate that adsorption is spontaneous and may be chemical in nature also, a positive value for the adsorption entropy which indicates that adsorbed dye molecules remain randomly on the adsorbent

References

1. Bhatnagar A.K., Jain A., comparative adsorption study with different industrial wastes as adsorbents for the removal of cationic dyes from water. *J Colloid Interface Sci*, 281, 49–55 (2005).
2. Vilaseca M., Gutie M.C., Grimau V.L., Mesas M.L., Crespi M., Biological treatment of a textile effluent after electrochemical oxidation of reactive dyes. *Water Environ Res*, 82, 176–181 (2010).
3. Awomeso J.A., Taiwo A.M., Gbadebo A.M., Adenowo J.A., Studies on the pollution of water body by textile industry effluents in Lagos, Nigeria. *J Appl Sci Environ Sanit*, 5, 353–359 (2010).
4. Brown D., Laboureur P., The aerobic biodegradability of primary aromatic amines. *Chemosphere*, 12, 405–414 (1983).
5. Tang W.Z., An H., UV/TiO₂ photocatalytic oxidation of commercial dyes in aqueous solutions. *Chemosphere*, 31, 4157 (1995).
6. Mohapatra P., Parida K.M., Photocatalytic activity of sulfate modified titania 3: decolorization of methylene blue in aqueous solution. *J Mol Catal A Chem*, 258, 118 (2006).
7. Lachheb H., Puzenat E., Houas A., Ksibi M., Photocatalytic degradation of various types of dyes (Alizarin S, Crocein Orange G, Methyl Red, Congo Red, Methylene Blue) in water by UV-irradiated titania. *Appl Catal B Environ*, 39, 75 (2002).
8. Robinson T., McMullan G., Marchant R., Nigam P., Remediation of dyes in textile effluent: a critical review on current treatment technologies with a proposed alternative. *Bioresour Technol*, 77 (3), 247–255 (2001).
9. Deans J.R., Dixon B.G., Uptake of Pb²⁺ and Cu²⁺ by novel biopolymers. *Water Res*, 26 (4), 469–472 (1992).
10. Nigam P., Armour G., Banat I.M., Singh D., Marchant R., Physical removal of textile dyes from effluents and solid-state fermentation of dye-adsorbed agricultural residues. *Bioresour Technol*, 72, 219–226 (2000).
11. Bhattacharyya K.G., Sharma A., Kinetics and thermodynamics of methylene blue adsorption on Neem (*Azadirachta indica*) leaf powder. *Dyes Pigments*, 65, 51–59 (2005).

12. Liao S., Chang W., Heavy metal phytoremediation by water hyacinth at constructed wetlands in Taiwan. *J Aqua Plant Manage*, 42, 60–68 (2004).
13. Jayaweera M.W., Kasturiarachchi J.C., Removal of nitrogen and phosphorus from industrial wastewaters by phytoremediation using water hyacinth (*Eichhornia crassipes* (Mart. Solms). *Water Sci Technol*, 50, 217–225.(2004).
14. Low C., Lee K., Tan K., Biosorption of basic dyes by water hyacinth roots. *Bioresour Technol*, 52, 79–83 (1995).
15. Gupta V.K., Ali I., Removal of Lead and Chromium From Wastewater Using Bagasse Fly Ash--A Sugar Industry Waste. *J Colloid Interface Sci*, 271 (2), 321–328 (2004).
16. Ahalya N., Kanamadi R.D., Ramachandra T.V., Biosorption of chromium (VI) from aqueous solutions by the husk of Bengal gram (*Cicer arietinum*), *Electron. J Biotechnol*, 8, 258–264 (2005).
17. Ali R.M., Hamada H.A., Hussein M.M., Malash G.F., potential of using green adsorbent of heavy metal removal from aqueous solutions: adsorption kinetics, isotherm, thermodynamic, mechanism and economic analysis. *Ecol Eng*, 91, 317–332 (2016).
18. Langmuir I., The adsorption of gases on plane surfaces of glass, mica and platinum, *J Am Chem Soc*, 40 (9), 1361–1403 (1918).
19. Shawabkeh R.A., Tutunji M.F., Experimental study and modeling of basic dye sorption by diatomaceous clay. *Appl Clay Sci*, 24, 111–120 (2003).
20. Lagergen S., “About the theory of so-called adsorption of soluble substances. *Handlingar Band*, 24 (4), 1.39 (1898).
21. Ho Y.S., McKay G., Pseudo-second order model for sorption processes. *Process Biochem*, 34, 451–465 (1999).
22. Maurya N.S., Mittal A.K., Cornel P., Rother E., Biosorption of dyes using dead macro fungi: effect of dye structure, ionic strength and pH. *Bioresour Technol*, 97, 512–521(2006).
23. Krishna L.S., Reddy A.S., Wan Zuhairi W.Y., Taha M.R., Reddy A.V., Indian jujuba seed powder as an eco-friendly and a low-cost biosorbent for removal of Acid Blue 25 from aqueous solution. *Sci World J*, (1), 1-12 (2014). doi.org/10.1155/2014/1840585
24. Hameed B.H., Din A.T.M., Ahmad A.L., Adsorption of methylene blue onto bamboo-based activated carbon: Kinetics and equilibrium studies. *J Hazard Mater*, 141, 819–825 (2007).
25. Yuh-Shan H.O., Isotherms for the Sorption of Lead onto Peat: Comparison of Linear and Non-Linear Methods. *Pol J Environm Stud*, 15(1), 81–86 (2006).
26. Hameed B.H., Mahmoud D.K., Ahmad A.L., Sorption of basic dye from aqueous solution by pomelo (*Citrus grandis*) peel in a batch system. *Coll Surf A*, 316(1–3), 78–84 (2008).
27. Mall I.D., Srivastava V.C., Agarwal N.K., Removal of Orange-G and methyl violet dyes by adsorption onto bagasse fly ash kinetic study and equilibrium isotherm analyses. *Dyes Pigm*, 69(3), 210–223 (2006).
28. Namasivayam C., Yamuna R.T., Adsorption of direct red 12 B by biogas residual slurry: Equilibrium and rate processes. *Environ Pollut*, 89, 1-7 (1995).
29. Rahchamani J., Zavvarmousavi H., Behzad M., Adsorption of methyl violet from aqueous solution by polyacryl amide as an adsorbent, isotherm and kinetic studies. *Desalination*, 267, 256–260 (2011).
30. Zine A.M., Thore S.N., Pawar R.P., Pardeshi S.D., Ligde N.M., Sonar J.P., Adsorption Studies of Acid Red 73 on *Parthenium hysterophorus* L. *IJCPS* 7 (4), 13-22 (2018).
31. Xing, Zengmeng; Tang, Bing; Chen, Xuan; Fu, Fenglian; Zhang, Zi; Lu, Zhigang, Effect of pore structure on the adsorption of aqueous dyes to ordered mesoporous carbons. *Microporous and Mesoporous Materials*, 227, 104-111 (2016).
32. Fu, Fenglian; Xiong, Ya; Xie, Baoping; Chen, Runming, Adsorption of Acid Red 73 on copper dithiocarbamate precipitate-type solid wastes. *Chemosphere*, 66 (1), 1-7 (2007).
33. Y.C. Wong a, Y.S. Szeto a, W.H. Cheung b, G. McKay b, Adsorption of acid dyes on chitosan—equilibrium isotherm analyses. *Process Biochemistry*, 39, 693–702 (2004).
34. Cheung a, Y.S. Szeto b, G. McKay a, Enhancing the adsorption capacities of acid dyes by chitosan nano particles. *Bioresource Technology*, 100, 1143–1148 (2009).